Porous Media", MS Thesis, Chem. Eng. Dept., Purdue Univ., Lafayette, IN (1969).
Paine, M. A., R. G. Carbonell, and S. Whitaker, "Dispersion in Pulsed Systems. Part I: Heterogeneous Reaction and Reversible Adsorption in a Capillary Tube," *Chem. Eng. Sci.*, 38, 1781 (1983).
Pfannkuch, H.-O., "Contribution à l'Etude des Déplacements des Fluides Miscibles dans un Milieu Poreux," *Revue de l'Institut du Pétrole*, **18**, 215 (1963).
Rifai, M. N. E., W. J. Kaufman, and D. K. Todd, "Dispersion in Laminar Flow through Porous Media", *Sanitary Eng. Res. Lab. Rpt. No. 3, IER Series* **90**, Berkeley, CA (July 1, 1956).
Ryan, D., R. G. Carbonell, and S. Whitaker, "A Theory of Diffusion and Reaction in Porous Media," *AIChE Symp. Ser., No. 202*, **77**, 46 (1981).
Saffman, P. G., "Dispersion in Flow through a Network of Capillaries," *Chem. Eng. Sci.*, **11**, 123 (1959).
Slattery, J. C., *Momentum, Energy, and Mass Transfer in Continua*, McGraw-Hill, New York (1972).
Taylor, G. I., "Dispersion of Soluble Matter in Solvent Flowing Slowly through a Tube," *Proc. Roy. Soc.*, **A219**, 186, London (1953).
———, "Conditions under Which Dispersion of a Solute in a Stream of Solvent Can be Used to Measure Molecular Diffusion," *Proc. Roy. Soc.*, **A225**, 473, London (1954).
Whitaker, S., "Diffusion and Dispersion in Porous Media," *AIChE J.*, **13**, 420 (1967).
Whitaker, S., "Forced Convection Heat Transfer Correlations for Flow in Pipes, Past Flat Plates, Single Cylinders, Single Spheres, and for Flow in Packed Beds and Tube Bundles," *AIChE J.*, **18**, 361 (1972).

Manuscript received April 11, 1983; revision received November 15, 1983, and accepted December 7, 1983.

Particle Collection in Magnetically Stabilized Fluidized Filters

A study was conducted on the use of magnetically stabilized fluidized (MSF) filters for removing fine particles from gases. The effect on filter performance of a number of variables was examined, including the applied field strength, gas velocities, and bed height. The dynamic behavior of MSF filters was found to be characterized by a decreasing collection efficiency with time as a result of significant particle re-entrainment.

R. V. ALBERT and CHI TIEN
Department of Chemical Engineering and Materials Science
Syracuse University
Syracuse, NY 13210

SCOPE

Granular filtration has been applied extensively in the past to control particulate emission and has proven effective for particles with a wide size range. It is particularly suitable for operation under high temperature and pressure conditions. On the other hand, granular filtration is inherently unsteady state. The accumulation of fine particles within a filter requires periodic media regeneration.

A possible way of overcoming the shortcomings arising from the cyclic nature of granular filtration is to operate filter beds in the fluidized mode, thus allowing a continuous withdrawal and introduction of filter grains. Furthermore, if fluidization is carried out with magnetic stabilization, the presence of gas bubbles in the bed can be eliminated and/or reduced. One may speculate that such an arrangement offers an ideal combination of high collection efficiency of granular filtration and the advantage of continuous operation, which is desirable in large-scale applications.

This paper reports results obtained from a systematic experimental study of the performance of magnetically stabilized fluidized (MSF) filters. The effect on filter performance of a number of variables was examined, including the magnetic field strength, gas velocities, bed height, and the size of fluidized particles. Experiments were also conducted on the extent of particle re-entrainment.

The concept of the unit collector efficiency proposed by Tien and Payatakes (1979) was used to assess the effectiveness of MSF filters and as a basis for comparing the performance of a MSF filter with its equivalent fixed-bed filter. The feasibility of employing a phenomenological rate expression to describe the dynamic behavior of MSF filters was also demonstrated.

CONCLUSIONS AND SIGNIFICANCE

The results of this experimental study demonstrate that substantial particle collection efficiency over long operating periods can be achieved with the use of fluidized filters under magnetic stabilization.

Compared with fixed-bed filters of comparable bed height, MSF filters give a somewhat lower collection efficiency. The most important variable affecting the performance of MSF filters is the applied magnetic field strength. Another important finding is the significant particle re-entrainment that occurs as the specific deposit of the filter increases. As a result, MSF filters, in most cases, exhibit a decrease in collection efficiency with time.

The dynamic behavior of MSF filters can be approximately described by the phenomenological equation for deep-bed filtration with the inclusion of particle re-entrainment.

INTRODUCTION

The first study on fluidized filtration was reported by Meissner and Mickley (1949) shortly after the introduction of fluidization in industrial application in 1942. Subsequent works (Anderson and Silverman, 1957; Scott and Guthrie, 1959; Pilney and Erickson, 1968; Knettig and Beeckmans, 1974; Doganoglu et al., 1978) have examined under a variety of conditions the removal from gases of particulates as well as mists and droplets. The possibility of enhancing particle collection by external forces (electrostatic and electromagnetic) have also been considered (Ciborovsky and Wlodarsky, 1961; Katz and Sears, 1969; Zahedi and Melcher, 1976, 1977).

One of the major disadvantages of fluidization is caused by the presence of gas bubbles. As shown in the work of Peters et al. (1982), the bubble phase of a fluidized filter offers a bypass for gas flow. Consequently, the overall collection efficiency of the filter is reduced. This shortcoming, of course, pertains to fluidized processing in general and is not confined only to filtration.

The possibility of suppressing bubble formation in a gas-solid fluidized bed by subjecting the bed to an external magnetic field has been explored by several investigators (Katz and Sears, 1969; Sonoliker et al., 1972; Ivanov and Shumkov, 1975). A more definitive study on stabilizing fluidization by magnetic force was recently done by Rosensweig (1978, 1979a, 1979b) and his co-workers (Lucchesi et al., 1979). As an approximation, a bed under magnetic stabilization can be viewed as homogeneous (uniform voidage), thus possessing certain intrinsic advantages to carry out contact processing.

Intuitively, one can readily see the advantages to be achieved if fluidized filters can be stabilized by external forces. Katz and Sears (1969), in their article, cited this improved collection efficiency as one of the several applications of stabilized fluidized beds. Similarly, Rosensweig, in his patent (1978), mentioned aerosol filtration as one possible application. Neither investigator, however, provided detailed information in this regard.

The purpose of this present work was to conduct a systematic experimental study of aerosol filtration in magnetically stabilized fluidized (MSF) filters and to examine, in some detail, the effects of various operating variables. The experimental results on particle collection were analyzed on the basis of the unit collector efficiency instead of the total collection efficiency, as has been the customary approach in the past. Thus, the efficiency of MSF filtration could be assessed in a more direct and meaningful manner.

EXPERIMENTAL WORK

Apparatus

The apparatus used in the experimental work is shown in Figure 1 and consists of the following:

Air Supply System. The air supply system was a Speedaire single-stage three-cylinder compressor (Model 3Z 170b, Dayton Electric Manufacturing Co.) equipped with an on-line dryer (Model 4Z 036). The dryer consisted of approximately 2×10^{-3} m^3 of Grade 42, Tel-Tale Silica gel dessicant supplied by Davison Chemical with an average particle diameter of 2.18 mm.

Aerosol Generating System. A TSI Model 3400 fluidized-bed aerosol generator was used to prepare the test suspensions used in the experiments. Talc powders were dispersed into the fluidized bed; the action of the fluidized particles dispersed the solid powders. The generator is capable of dispersing particles of the size range of 0.1 to 25 μm dia. and has a capacity of 0.35 ~ 35 mg/cm^3.

The air supplied by the compressor passed first through a rotameter and was then divided into two parts. Part of the air was used to operate the aerosol generator. The exit air stream from the aerosol generator was then combined with the rest of the air supply, entering a mixing chamber that consisted of a plexiglass column with four baffles. Finally, the air supply passed into the MSF filter.

MSF Filter Bed. The MSF filter was made of a plexiglass column (50.8 mm dia. 731.8 mm height). The gas distributor was a 22-gauge A.W.G. wire screen with 0.325 mm openings. Below the distributor was a sampling port

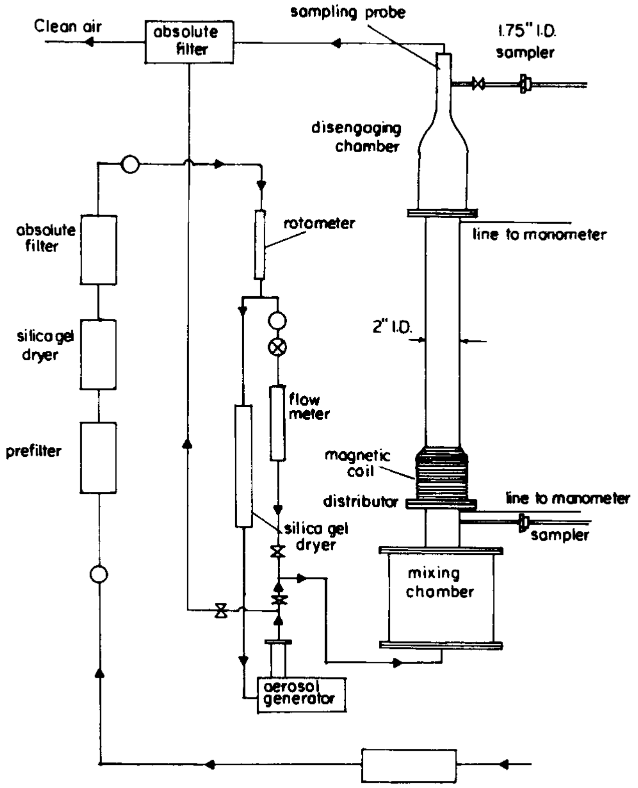

Figure 1. Schematic diagram of the experimental apparatus.

from which the influent aerosol samples were taken. A disengaging chamber was used to remove elutriated particles (magnetite) from the exit air. At the outlet of the MSF filter was another sampling port for taking effluent air samples.

The magnetic field for stabilizing fluidization was provided by a magnetic coil placed outside the filter. The coil, which had a diameter of approximately 83 mm, consisted of a total of 488 m of 9-gauge wire A.W.G., wrapped evenly over a 152.4 mm section of the filter bed. Electric power was supplied from a Viz WP-707 direct-current power Supplysts with a maximum capacity of 1.47 amps of direct current.

Sampling System. The influent and effluent aerosol concentrations were determined by weighing particles retained by a Gelman glass-fiber filter paper. The sample holders which housed the filter paper were made from ½-inch (12.7 mm) compressed air unions with ½- to ¼-inch (12.7 to 6.35 mm) reducers at each end, combined with ¼-inch (6.35 mm) tubing connectors. Inside the union, a stainless steel screen as attached and used as the filter paper support.

Experimental Systems

Magnetite particles (Fe_3O_4) supplied by N/L Chemical, McIntyre Division, Tahawus, NY, were used as filter grains in the MSF filters. Three sizes were used, most frequently particles with an average size of 529 μm. Table 1 lists the relevant properties of the magnetite particles as well as the range of operating conditions.

Talc powder of a chemical composition approximated by the formula $Mg_6(Si_2O_5)_4(OH)_4$ was used as aerosol particles. The talc powder size, determined by microscopic observation, was 1.9 μm dia. with a log-normal deviation of 2.2 for the effluent stream, and 2.0 μm dia. with a log-normal deviation of 2.1 for the influent stream. The aerodynamic diameters of aerosol particles were found to be 2.405 μm and 2.320 μm for the effluent and influent, respectively. These measurements were done under the following conditions: bed height, 0.111 m; magnetite particles, dg = 529 μm; u_s = 0.369 m/s; and without any applied magnetic field.

Procedures

Prior to each filtration experiment, the following steps were taken: fresh dry silica gel was placed in the air dryer; the proper amount of Gelman glass-fiber filters (Type A, product #61701) were cut and weighed for sampling, and finally magnetite particles were charged into the MSF filter.

After completing these steps, the aerosol generator was started and al-

TABLE 1. EXPERIMENTAL CONDITIONS

Magnetite used as Filter Grams

Tyler Mesh	Avg. Dia., μm	Porosity	Min. Fluidization Velocity U_{mf}, m/s
14–24	1,217	0.539	0.446
24–48	529	0.501	0.206
48–150	260	0.471	0.093

Talc Powder Diameter, μm

	Aerodynamic	Microscopic
Inlet	2.320	2.000 log-normal dispersion = 2.1
Outlet	2.405	1.9 log-normal dispersion = 2.2

Gas Velocity, m/s
0.213, 0.233, 0.252, 0.272, 0.311
0.369, 0.427, 0.504, 0.590, 0.671
0.749

Particle Sizes, μm
260, 529, 1,217

Bed Heights, m
0.014, 0.025, 0.028, 0.056
0.083, 0.111

lowed to run until its operation reached a steady state. The steady-state condition was determined by observations through a window on the side of the generator. Here one could see whether a steady stream of talc powder was rising out of the generator, rather than either clear air or agglomerates of powder sticking to the side of the window. Once the steady state was reached, the aerosol suspension was allowed to pass through the filter with the magentic field turned on. Aerosol samples were taken simultaneously at both the inlet and the exit of the filter at a flow rate isokinetic to that at the filter inlet. The samples were taken every 30 minutes; the time required for replacing filter papers in sample holders was approximately two minutes. Each experiment lasted approximately three to four hours.

To measure re-entrainment, after a significant decline in collection efficiency was observed the aerosol generator was turned off, but air flow through the filter was maintained and effluent sampling was continued as before for approximately three more hours.

In addition to the filtration and re-entrainment experiments, measurements were also taken of the velocity as a function of the applied magnetic field strength, H, for stabilizing fluidization. These measurements were made by adjusting the magnetic field strength while keeping air flow (without talc powder) through the MIS filter at a specified rate. Stability was taken to be the point where bubbling was barely observed. This information was used to obtain the stability diagrams for the bed.

Experimental Variables

The experimental variables considered in this work include the media height (expressed in terms of the equivalent fixed-bed height), the applied magnetic field strength, the size of magnetite particles (filter grains), and the gas velocities. The stability condition of the experimental filter ranged from being highly stable to marginally stable to unstable—that is, with insufficient magnetic field strength or no magnetic field.

A total of 78 runs were made. A summary of the experimental conditions is given in Table 1. The data are tabulated in Albert (1982).

RESULTS

Stability Diagrams

In order to properly carry out the experimental work and to subsequently interpret the results, it was necessary to identify the condition which produces stabilized fluidization. The criterion which determines the onset of instability in a gas-solid fluidized bed in the presence of a magnetic field was determined by Rosensweig (1979a). It is based on a linear stability analysis and gives the following results:

$$N_m N_v > 1 \text{ unstable} \tag{1}$$

$$N_m N_v < 1 \text{ stable} \tag{2}$$

The dimensionless parameters N_m and N_v are defined as

$$N_m = \frac{\rho_p u}{M^2} \tag{3}$$

$$N_v = \frac{4\pi(3-2\epsilon)^2}{\epsilon^2(1-\epsilon)}[1 + (1-\epsilon)x_o - (1-\epsilon)(x_o - \hat{x}_o)\cos^2\theta]\frac{\cos^2\gamma}{\cos^2\theta} \tag{4}$$

where ρ_p is the density of the fluidized particles, ϵ is the bed porosity, and u is the superficial velocity. M denotes solids magnetization and is a function of the applied magnetic field. The angles γ and θ are, respectively, that between the direction of the gas flow and the direction of the wave disturbance, and that between the magnetic field and the wave disturbance. The solids magnetization, M, can be written as

$$M = x_o H \tag{5}$$

where H is the strength of the magnetic field and x_o is the chord susceptibility.
The quantity $\hat{x}_o$, the tangent susceptibility, is given as

$$x_o = \frac{dM}{dH} \tag{6}$$

The maximum value of N_v occurs at $\gamma = 0$, namely a disturbance wave oriented along the axial direction of the bed. This disturbance can best be suppressed if the direction of the applied magnetic field coincides with that of the disturbance wave. Accordingly, N_v becomes

$$N_v = \frac{4\pi(3-2\epsilon)^2}{\epsilon^2(1-\epsilon)}[1 + (1-\epsilon)\hat{x}_o] \tag{7}$$

At the marginal state,

$$N_m N_v = 1$$

and

$$N_m = N_v^{-1} = \frac{\epsilon_o^2(1-\epsilon_o)}{4\pi(3-2\epsilon_o)^2[1 + (1-\epsilon_o)\hat{x}_o]} \tag{8}$$

where the subscript o denotes the marginal state. The above expression, together with the definition of N_m (i.e., Eq. 3) can be rewritten as

$$\frac{M_o}{\rho_p^{1/2} u_{mf}} = N_m^{-1/2}\frac{u_o}{u_{mf}} = N_v^{1/2}\frac{u_o}{u_{mf}} \tag{9}$$

when u_{mf} is the minimum fluidization velocity.

Assuming that the Carman-Kozeny equation applies to a magentically stabilized bed at its marginal state, one may write

$$\frac{u_o}{u_{mf}} = \frac{\epsilon_o^3}{(1-\epsilon_o)}\frac{(1-\epsilon_d)}{\epsilon_d^3} \tag{10}$$

where ϵ_d is the porosity of the bed corresponding to the minimum fluidization condition. Substituting Eq. 7 and 10 into 9, one has

$$\frac{M_o}{\rho_p^{1/2} u_{mf}} = \frac{\{4\pi[1 + (1-\epsilon_o)x_o]\}^{1/2}(3-2\epsilon_o)\epsilon_o^2(1-\epsilon_d)}{(1-\epsilon_o)^{3/2}\epsilon_d^3} \tag{11}$$

Thus, from the experimental data of u_o vs. ϵ_o, the curve of u_o/u_{mf} vs. $M_o/\rho_p^{1/2}u_{mf}$, which separates the region of stability from that of instability, can be constructed with the assumption that $x_o = 1$. An example of this stability curve is shown in Figure 2.

Data Representation

The measurements obtained in the filtration experiments are the influent and effluent concentrations, c_{in} and c_{eff}, expressed as mg talc powder per m^3 of air at various times. The total collection efficiency of the filter at any time, E, is defined as

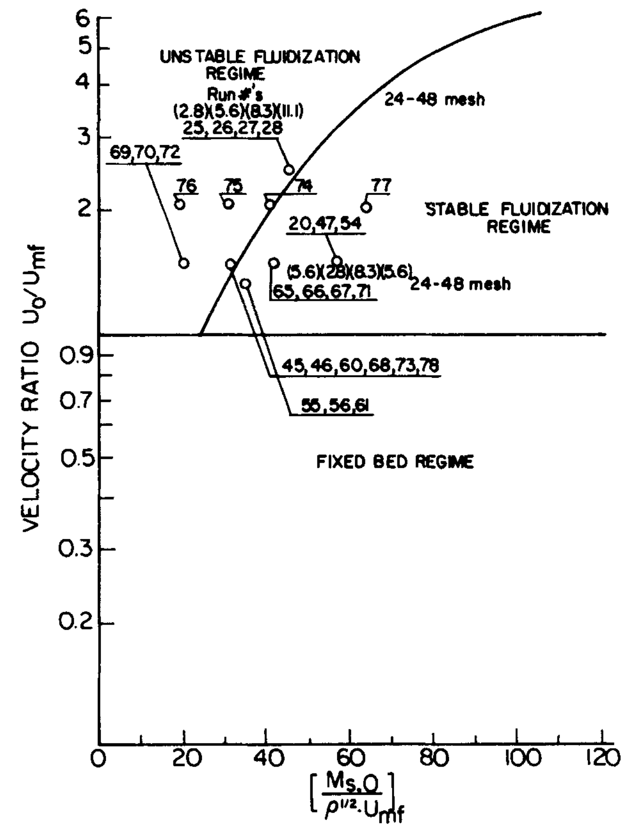

Figure 2. Stability diagram for bed height experiments with 24–48 Tyler mesh particles.

$$E = \frac{c_{in} - c_{eff}}{c_{in}} \tag{12}$$

While it is customary to express the dynamic behavior of filters by the variation of E with time, the fact that the influent concentration was only approximately constant (as a result of the limitations of the aerosol generator) suggests that it is more proper to express E against the total number of particles collected by the bed, m (mg of particles). The latter quantity can be evaluated as

$$m = \int_o^t (c_{in} - c_{eff})(u)(A)dt \tag{13}$$

The total collection efficiency, however, does not provide a direct measurement of the particle-collecting capability of the filter bed. A quantity found to be useful in characterizing the particle-collecting capability of a fixed-bed filter is the so-called filter coefficient, λ. For a fixed bed of uniform porosity of height L, the total collection efficiency, E, can be written as

$$E = 1 - \frac{c_{eff}}{c_{in}} = 1 - \exp[-\lambda L] \tag{14}$$

If one considers magnetically stabilized fluidized beds to be in a state of homogeneous fluidization, then Eq. 14 should be applicable to MSF filters as well. For consistency of comparison, L may be taken to be the bed height corresponding to the condition at incipient fluidization, L_{mf}. The actual bed height of the MSF filter may be different from L_{mf}; however, the difference is too small to be significant.

The filter coefficient, λ, can in turn be related to the unit collector efficiency, η, by the expression of Payatakes et al. (1974):

$$\eta = (\lambda)(l_c) \tag{15}$$

where l_c is the axial distance corresponding to a unit collector and, according to Payatakes et al. (1973), is given as

$$l_c = d_g \left[\frac{\pi}{6}\frac{1}{1-\epsilon}\right]^{1/3} \tag{16}$$

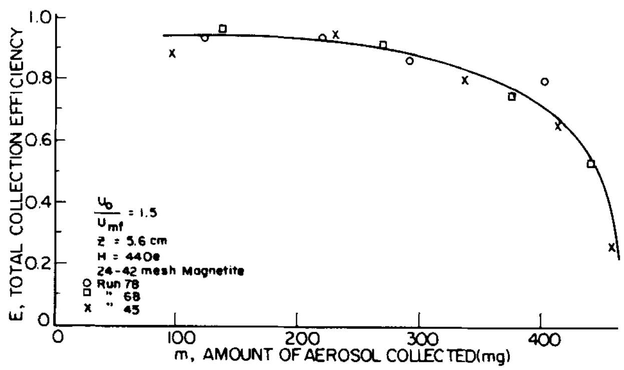

Figure 3. Demonstration of data reproducibility.

Data Reproducibility

The reproducibility of the filtration experiment is shown in Figure 3, in which the experimentally determined total collection efficiency is presented as a function of total dust loading of the filter, m. The results shown in this figure were obtained under marginal stable conditions. Similar results were also obtained with the application of different magnetic field strength.

Effect of Magnetic Stabilization

Among the variables investigated, the most important was the strength of the applied magnetic field. The total collection efficiency was found to increase dramatically as the bed became stabilized and the state of fluidization changed from the bubble regime to the homogeneous regime. The data shown in Figure 4 are a good example. The results shown in this figure are those obtained from three runs corresponding to (a) without magnetic field, (b) with magnetic field but unstable, and (c) with magnetic field and stable.

Effect of Gas Velocity

In fixed-bed granular filtration, the effect of particle inertia on collection is important. One expects an increase in collection efficiency at higher gas velocities. For fluidized filters, this inertial effect is also anticipated, although to a lesser extent. On the other hand, at higher gas velocities the fraction of gas which passes through the bed in the form of gas bubbles increases. As the extent of gas bypassing increases, so does the reduction in the overall collection efficiency. This adverse effect of high gas velocity often outweighs its benefits.

The experimental results shown in Figure 5a serve to illustrate this point. These experimental runs were conducted with the same applied magnetic field strength but at different gas velocities. Specifically, run 1 was made under stable conditions. The total collection efficiency decreased significantly as the gas velocities increased. This situation provides a good indication of the signifi-

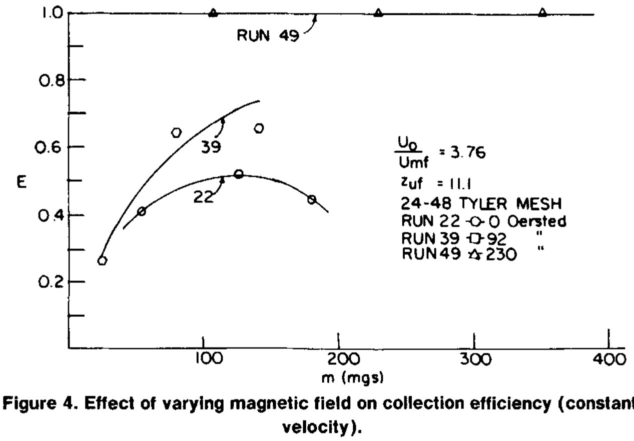

Figure 4. Effect of varying magnetic field on collection efficiency (constant velocity).

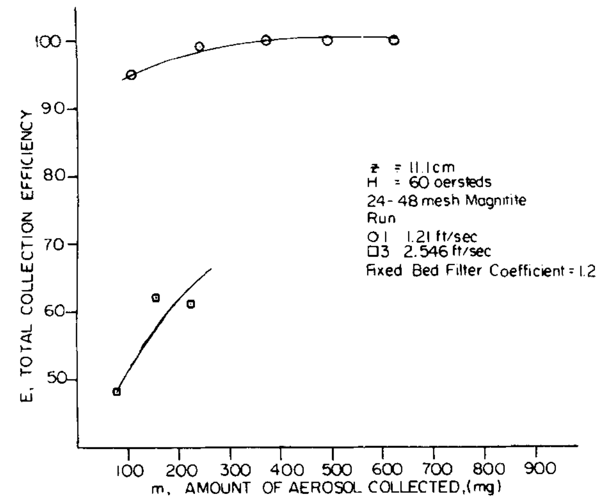

Figure 5a. Effect of magnetic stabilization on collection efficiency.

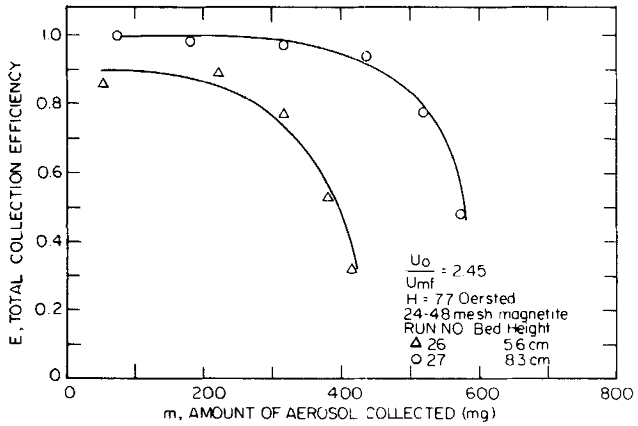

Figure 5b. High gas velocity (marginally stable bed).

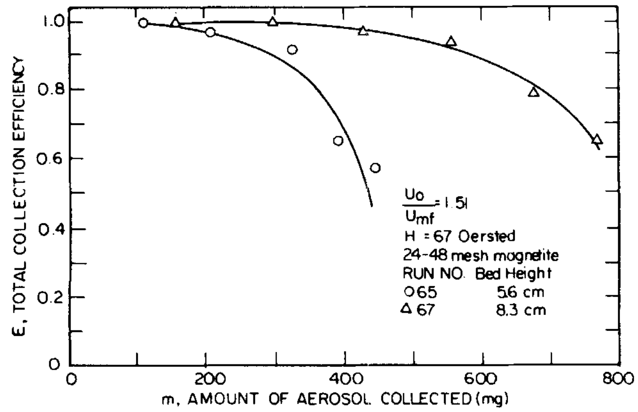

Figure 5c. Low gas velocity (stable bed).

cant influence of gas bypassing on the performance of fluidized filters.

It is also interesting to examine the effect of gas velocity on stabilized fluidized beds by comparing the results of runs 25 and 26 with runs 65 and 67. As shown in the stability diagram (Figure 2), both sets of experiments were conducted with similar magnetic fields, but the former set (runs 25 and 26) had a much higher velocity than the latter. As a result, the conditions of runs 25 and 26 correspond to the marginal state, while those of runs 65 and 67 are well within the stability range. The results of the total collection obtained, as shown in Figures 5b and 5c, indicate that higher gas velocity did not yield better particle collection. This point will be discussed below.

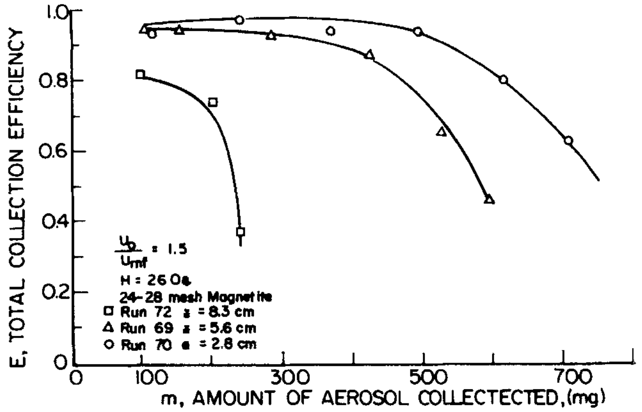

Figure 6. Effect of bed height on total collection efficiency (unstable fluidization).

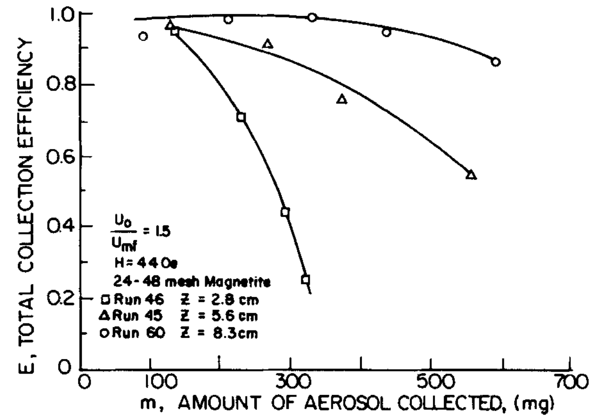

Figure 7. Effect of bed height on total collection efficiency (marginal state).

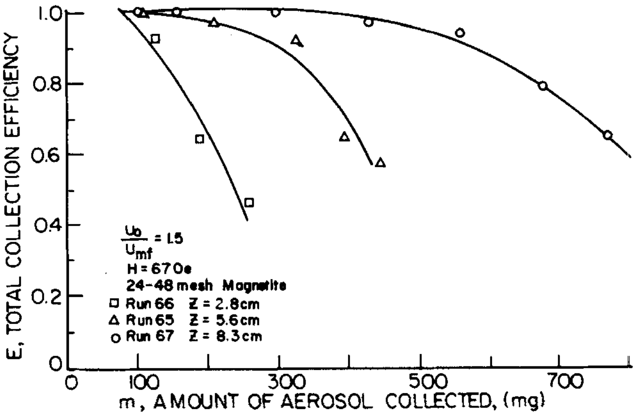

Figure 8. Effect of bed height on total collection efficiency (stable fluidization).

Transient Behavior

The time-dependent behavior of MSF filters is shown in Figures 6–10. In these figures, the results of the total collection efficiency are shown as a function of the total number of particles collected for filters of different bed heights operating at similar conditions. The conditions under which the results shown were obtained ranged from unstable (outside stability region) to highly stable, the latter of which was achieved by increasing the applied magnetic field strength while keeping the gas velocity constant. Runs 25–28, the results of which are given in Figure 10 were conducted at a higher gas velocity than those used in collecting results shown in Figures 6–9 and the state of fluidization was stable.

In spite of the fluctuations shown in these figures, some general trends can be discerned. The total collection efficiencies obtained

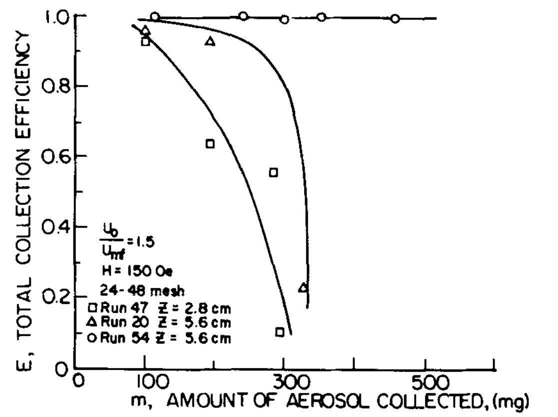

Figure 9. Effect of bed height on total collection efficiency (highly stabilized).

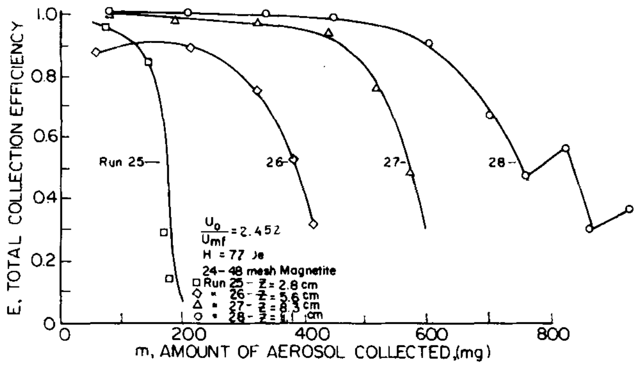

Figure 10. Effect of bed height on total collection efficiency.

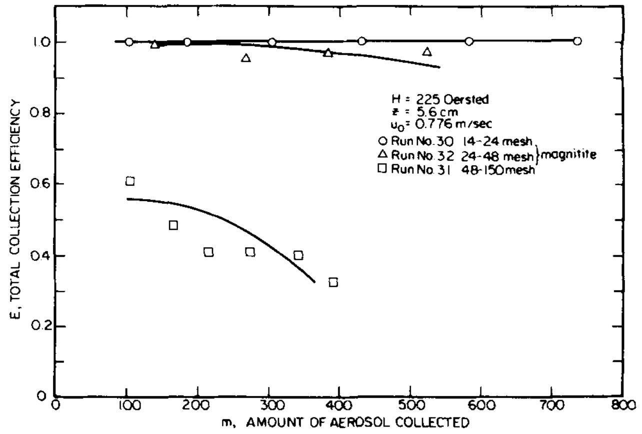

Figure 11. Effect of particle size on collection efficiency.

display consistency with respect to bed height. Generally speaking, E was found to decrease with the amount of the aerosol collected or with time. For long beds (0.111 m), this decrease is gradual and does not begin until the values of m become large. In contrast, for shallow beds the decrease in E occurred rather early and fairly rapidly. This behavior is true for all sizes of magnetite used. At the highest velocity examined, the collection efficiency obtained was found to be inferior to that of the corresponding fixed bed. This finding can be seen most clearly by noting the fact that a filter of 529 μm magnetite with a bed height of 0.028 m operating at a velocity below minimum fluidization (i.e., in fixed-bed mode) gave almost complete particle collection (Albert, 1982).

In addition to their decrease in total collection with time, MSF filters also exhibit two other special features. The first feature can be seen from the results shown in Figures 7 and 10. These figures give the results obtained under the marginally stable conditions shown in Figure 2. When the collection efficiencies were compared, however, the values shown in Figure 7 are, in general, greater than those in Figure 10 for the same bed height. This comparison, together with the results mentioned earlier, is contrary to the well-known fact that in fixed-bed filtration particle collection improves with the increase in particle inertia.

The second special feature can be seen by comparing the curves shown in Figure 11. These results were obtained using comparable gas velocities (0.776 m/s) but significantly different-size magnetite particles. According to most fixed-bed collection efficiency correlations, the smaller particle is expected to give higher collection efficiencies, which is obviously contrary to the results shown in these figures.

The decrease in collection efficiency with time can be explained to a degree by particle re-entrainment, which will be discussed in a following section.

Comparison with Fixed-Bed Performance

To obtain a measure of the effectiveness of MSF filtration, one may compare the performance of an MSF filter to the performance of an identical filter operated in the fixed-bed mode, namely by comparing the manner in which the filter coefficient varied with the extent of particle deposition in these three cases. The extent of deposition can be described by the specific deposit, σ, defined as the mass of particles collected per unit volume of filter bed. Experimentally, σ may be taken to be

$$\sigma = m/V \tag{17}$$

where m is the total number of particles collected in the filter and V is the volume of the filter based on the bed height at the onset of fluidization, L_{mf}. The use of Eq. 17 is based on the assumption that particle collection within the filter bed is uniform.

Figures 12 and 13 show two sets of experimental results for λ vs. σ. The degree of the dependence of λ on σ was found to vary with bed height. For bed height greater than 5.6 cm, the scattering of data was such that one may conclude that a single relationship of λ vs. σ holds true for all bed heights.

The filter coefficient of a fixed bed can be estimated from Eq. 15 and the Pendse-Tien (1982) correlation, that is

$$\eta = (1 + 0.04\, N_{Re,s}) \left[N_{st} + \left\{ 0.48 \left(4 - \frac{4N_R}{d_c^*} - \frac{N_R^2}{d_c^{*2}} \right)^{1/2} \left(\frac{N_R^{1.041}}{d_c^*} \right) \right\} \right] \tag{18}$$

where $N_{Re,s}$, N_{St}, and N_R are the Reynolds, the Stokes, and the relative size parameters (their definitions are given in the notation); d_c^* is the dimensionless constriction diameter, which can be determined from the capillary pressure-saturation measurement (Payatakes et al., 1973). As an approximation, d_c^* may be assumed to be 0.35.

Two conclusions can be inferred from these measurements. First, the unit collector efficiency of MSF filters exhibits time-dependent behavior and, by and large, η decreases with σ. This behavior is in conflict with the well-established fact that the unit collector efficiency, η, increases with σ. This apparent contradiction can be reconciled, however, if the effect of particle re-entrainment is considered. This point will be discussed further in the following section.

The second conclusion is that the performance of an MSF filter can be approximated, as an upper limit, by the performance of an equivalent fixed-bed filter (i.e., an identical fixed-bed filter, operating at the same gas velocity). This conclusion is based on the fact that the experimentally determined filter coefficient, in all cases considered, was found to be less than the value estimated from Eqs. 15 and 18. Furthermore, as the degree of bed stabilization increases, the degree of approximation also improves. This point can be seen from Figure 14, in which the results from two experimental runs (65 and 69) are displayed. The data for λ vs. σ from run 65 corresponding to stable fluidization, when extrapolated to zero time (i.e., σ = 0), yielded a value much closer to the corresponding fixed-bed value than did that of run 69, which was made outside the stability region (see Figure 2).

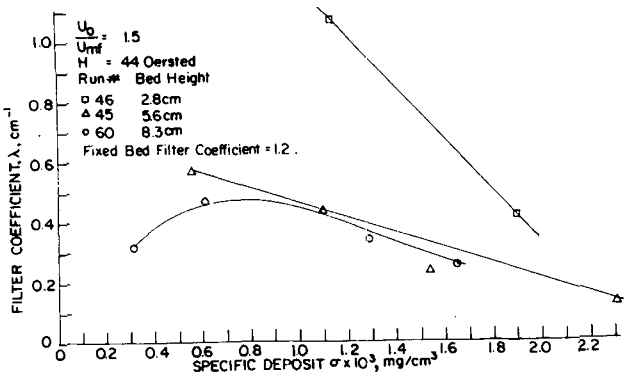

Figure 12. Filter coefficient λ vs. specific deposit σ.

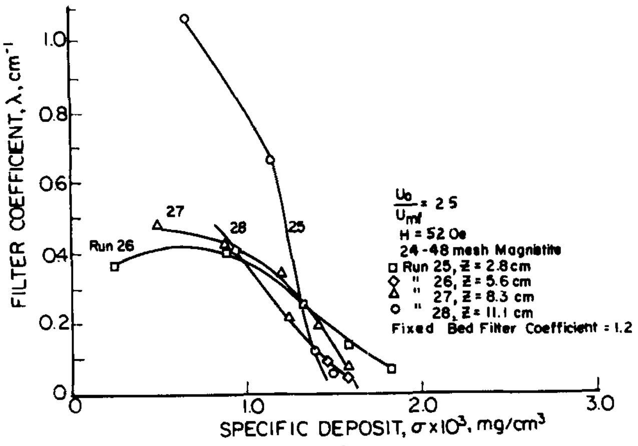

Figure 13. Filter coefficient λ vs. specific deposit σ.

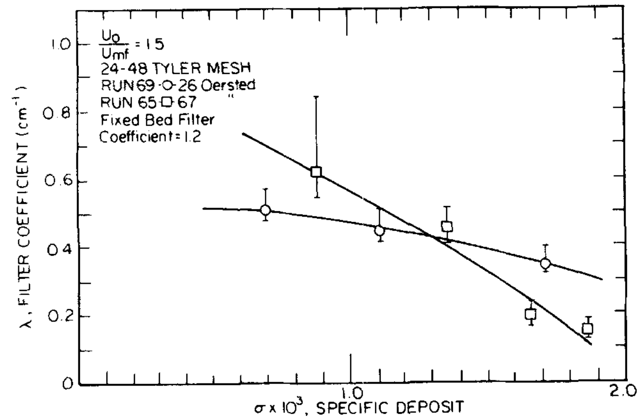

Figure 14. Magnetic field is varied, inside and outside stability region.

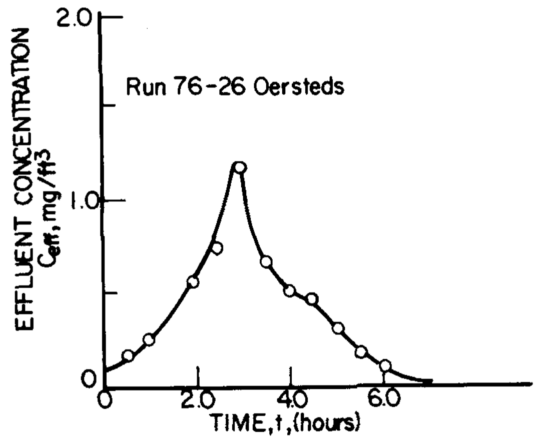

Figure 15. Effluent concentration vs. time for re-entrainment experiments.

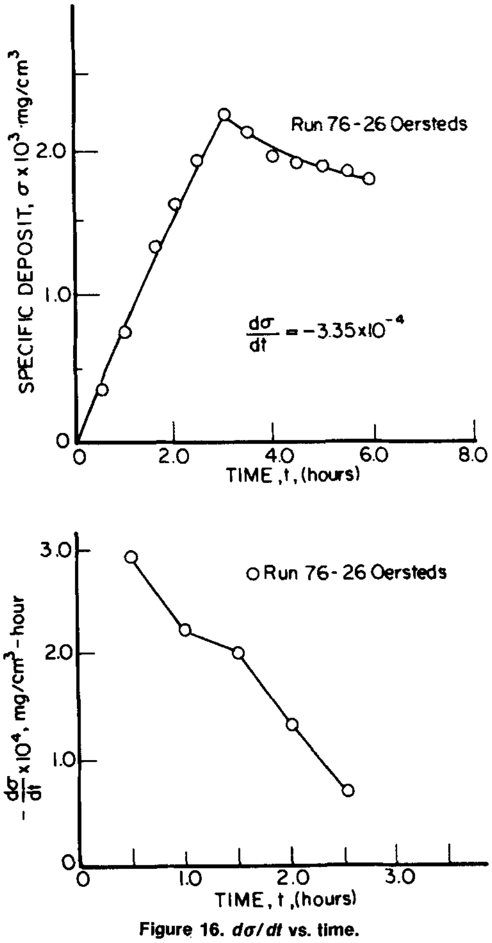

Figure 16. $d\sigma/dt$ vs. time.

Particle Re-entrainment

Most of the particle re-entrainment experiments were conducted with a bed height of 0.056 m and at different gas velocities and magnetic field strengths. As an example, the results of run 76 are shown in Figure 15; here the effluent concentration is shown as a function of time. Initially, the effluent particle concentration history increases steadily, which corresponds to the filtration phase of the measurement and is consistent with the results shown earlier. After the point at which the aerosol generator was shut off, the effluent particle concentration decreases with time. The corresponding values of the specific deposit, σ, and the rate of the change of σ, $d\sigma/dt$, were calculated from the effluent particle concentration data with the use of Eqs. 12 and 16 and are also shown in Figure 16.

A preliminary attempt was made to incorporate the effect of particle re-entrainment in describing the performance of MSF filters. The filtration rate equation (Tien and Payatakes, 1979) can be written as

$$\frac{1}{u}\left(\frac{\partial\sigma}{\partial\theta}\right) = -\left(\frac{\partial c}{\partial z}\right) = \lambda_o c - (k/u) \tag{19}$$

where λ_o is the initial filter coefficient and k is the rate of particle reentrainment. The two independent variables, z and θ, are respectively, the axial bed distance and corrected time, defined as $t - z\epsilon/u$.

The solution to Eq. 19 is

$$c = \left[c_{\text{in}} + \frac{1}{u}\int_o^z e^{\lambda_o z} k dz\right] e^{-\lambda_o z} \tag{20}$$

During the re-entrainment phase of the measurement, $c_{\text{in}} = 0$. An average value of k over the entire bed can be found from the

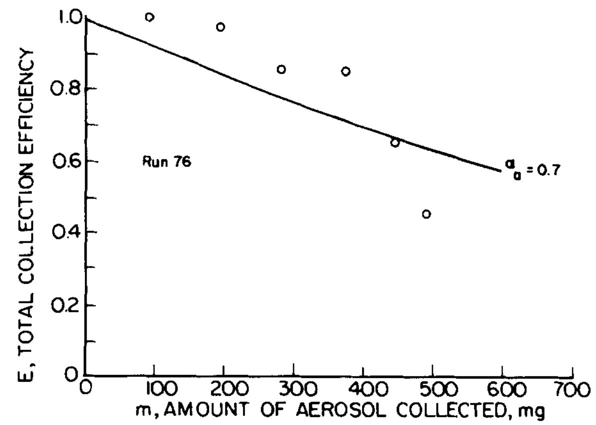

Figure 17. Comparison between prediction and experiment.

effluent concentration measurement by applying Eq. 20 to $z = L_{mf}$. After rearrangement, one has

$$k = \frac{c_{\text{eff}} u \lambda_o}{1 - \exp[-\lambda_o L_{mf}]} \tag{21}$$

From physical ground, it is necessary to relate the rate of re-entrainment to the extent of particle deposition, i.e., σ. As an extreme simplification, o may assume

$$k = \alpha_a \sigma \tag{22}$$

namely, that the rate of re-entrainment is directly proportional to σ.

A prediction of filter performance including the re-entrainment effect corresponding to the experimental condition of run 76 was made and the results are shown in Figure 17. Although this agreement by no means can be considered good, the deterioration in total collection efficiency was observed correctly.

ACKNOWLEDGMENT

This study was performed under control No. DE-AC02-79-ER-10386, Department of Energy, Office of Basic Energy Sciences.

NOTATION

A = cross-sectional area of filter
C = particle concentration
$c_{\text{eff}}, c_{\text{in}}$ = effluent and influent particle concentration respectively
c_s = Cunningham's correction factor
d_g = filter grain diameter
d_p = particle diameter
d_c^* = dimensionless pore constriction diameter
E = total collection efficiency
H = magnetic field strength
k = rate of particle re-entrainment
L = bed height
L_{mf} = bed height at the incipience of fluidization
l = axial distance of a unit collector
M = magnetization of fluidized particles
M_o = value of M at marginal state
m = number of particles collected in filter
N_m = dimensionless parameter defined by Eq. 3
N_v = dimensionless parameter defined by Eq. 4
N_R = relative size parameter defined as d_p/d_g
$N_{Re,s}$ = Reynolds number defined as $d_g u \rho/\mu$
N_{St} = Stokes number defined as $d_p^2 u \rho_p C_s/\mu d_g$
t = time
u = superficial gas velocity
u_o = value of u at marginal state
u_{mf} = minimum fluidization velocity
V = volume of filter
x_o = chord susceptibility
$\hat{x}_o$ = tangent susceptibility
z = axial distance

Greek Letters

α_a = constants of Eq. 22
ϵ = porosity of bed
ϵ_d = porosity of a filter bed at packed bed state
ϵ_o = value of ϵ at marginal state
ρ = gas density
ρ_p = particle density
λ = filter coefficient
λ_o = initial filter coefficient
σ = specific deposit
γ = angle between the direction of gas flow and that of wave disturbance
θ = corrected time, or angle between direction of wave disturbance and direction of applied magnetic field
μ = gas viscosity

LITERATURE CITED

Albert, R. V., "Dust Filtration with a Magnetically Stabilized Fluidized Bed," MS Thesis, Syracuse Univ., Syracuse, NY (1982).

Anderson, D. M., and L. Silverman, "Isokinetic Sampling Probes," Paper presented at the 5th Air Cleaning Seminar, Harvard Public School of Health, Boston (1979).

Ciborovsky, J., and A. Wlodansky, "On Electrostatic Effects in Fluidized Beds," *Chem. Eng. Sci.*, **17**, 23 (1962).

Doganoglu, Y., et al., "Removal of Fine Particulates from Gases in Fluidized Beds," *Trans. I. Chem. Eng.*, **576**, 239 (1978).

Ivanov, D. G., and S. Kh. Shumkov, "Investigation of the Heterogeneity of a Fluidized Bed of Catalyst for the Synthesis of Ammonia in a Electromagnetic Field," *Int. Chem. Eng.*, **15**, 557 (1975).

Katz, H., and J. T. Sears, "Electric Field Phenomena in Fluidized and Fixed Beds," *Can. J. Chem. Eng.*, **47**, 50 (1969).

Knettig, P., and J. M. Beeckmans, "Capture of Monodispersed Aerosol Particles in a Fixed Bed and in a Fluidized Bed," *Can. J. Chem. Eng.*, **52**, 703 (1974).

Lucchesi, P. J., et al., "Magnetically Stabilized Beds: New Gas-Solids Contacting Technology," 10th World Petroleum Cong., Bucharest (1979).

Meissner, H. P., and H. S. Mickley, "Removal of a Mist in a Fluidized Bed," *Ind. Eng. Chem.*, **41**, 1,238 (1949).

Payatakes, A. C., C. Tien, and R. M. Turian, "A New Model for Granular Porous Media. I: Model Formulation," *AIChE J.*, **19**, 58 (1973).

———, "Trajectory Calculation of Particle Deposition in Deep Bed Filtration," *AIChE J.*, *20*, 889 (1974).

Pendse, H., and C. Tien, "General Correlation of the Initial Collection Efficiency of Granular Filter Beds," *AIChE J.*, *28*, 677 (1982).

Peters, M. H., L. S. Fan and T. L. Sweeney, "Simulation of Particulate Removal in Gas Solid Fluidized Beds," *AIChE J.*, **39** (1982).

Pilney, J. P., and E. E. Erickson, "Fluidized Bed Fly Ash Filter," *J. Air Pollut. Cont. Assoc.*, **16**, 684 (1984).

Rosensweig, R. E., "Process for Operating a Magnetically Stabilized Fluidized Bed," U.S. Patent No. 4,115,927 (1978).

———, "Fluidization Hydrodynamic Stabilization with a Magnetic Field," *Science*, **204**, 57 (1979a).

———, "Magnetic Stabilization of the State of Uniform Stabilization," *Ind. Eng. Chem. Fund.*, **18**, 260 (1979b).

Scott, D. S., and D. A. Guthrie, "Removal of a Mist in a Fluidized Bed," *Can. J. Chem. Eng.*, **200** (1959).

Sonoliker, R. L., et al., "Influence of Magnetic Field on Fluidization of Iron Particles," *Indian J. Tech.*, **10**, 377 (1972).

Tien, C., and A. C. Payatakes, "Advances in Deep Bed Filtration," *AIChE J.*, **25**, 737 (1979).

Zahedi, D., and J. R. Melcher, "Electrofluidized Beds in the Filtration of a Submicron Aerosol," *J. Air Pollution Control Ass.*, **26**, 345 (1976).

———, "Collection of Submicron Particles in Bubbling Electrofluidized Beds," *Ind. Eng. Chem. Fund.*, **16** (1977).

Manuscript received April 27, 1983; revision received November 18, 1983, and accepted December 6.